A Solar Based Power Module for Battery-Less IoT Sensors Towards Sustainable Smart Cities

Saswat Kumar Ram[1], Shubham Chourasia[1], Banee Bandana Das[1], Ayas Kanta Swain[1], Kamalakanta Mahapatra[1], and Saraju P. Mohanty[2]

[1]National Institute of Technology, Rourkela, India
[2]University of North Texas, USA.

Email ID: saswatram01@gmail.com

Outline

- Introduction
- Novel Contribution of this Paper
- Proposed SEHS-PMU
- Simulation Results
- Conclusion and Future Directions
- References

Introduction

- Most of the edge devices (sensors) are battery powered and are always active, which puts the stress on battery-based power supply.
- Availability of natural resources for energy harvesting as solar, thermal, microbial, vibration and RF (radio frequency).
- An Efficient Power Management Mechanism improves the performance in IoTs.
- Solar Energy Harvesting System (EHS) is a well-suited alternative to power IoT end node devices.

Introduction Cond..

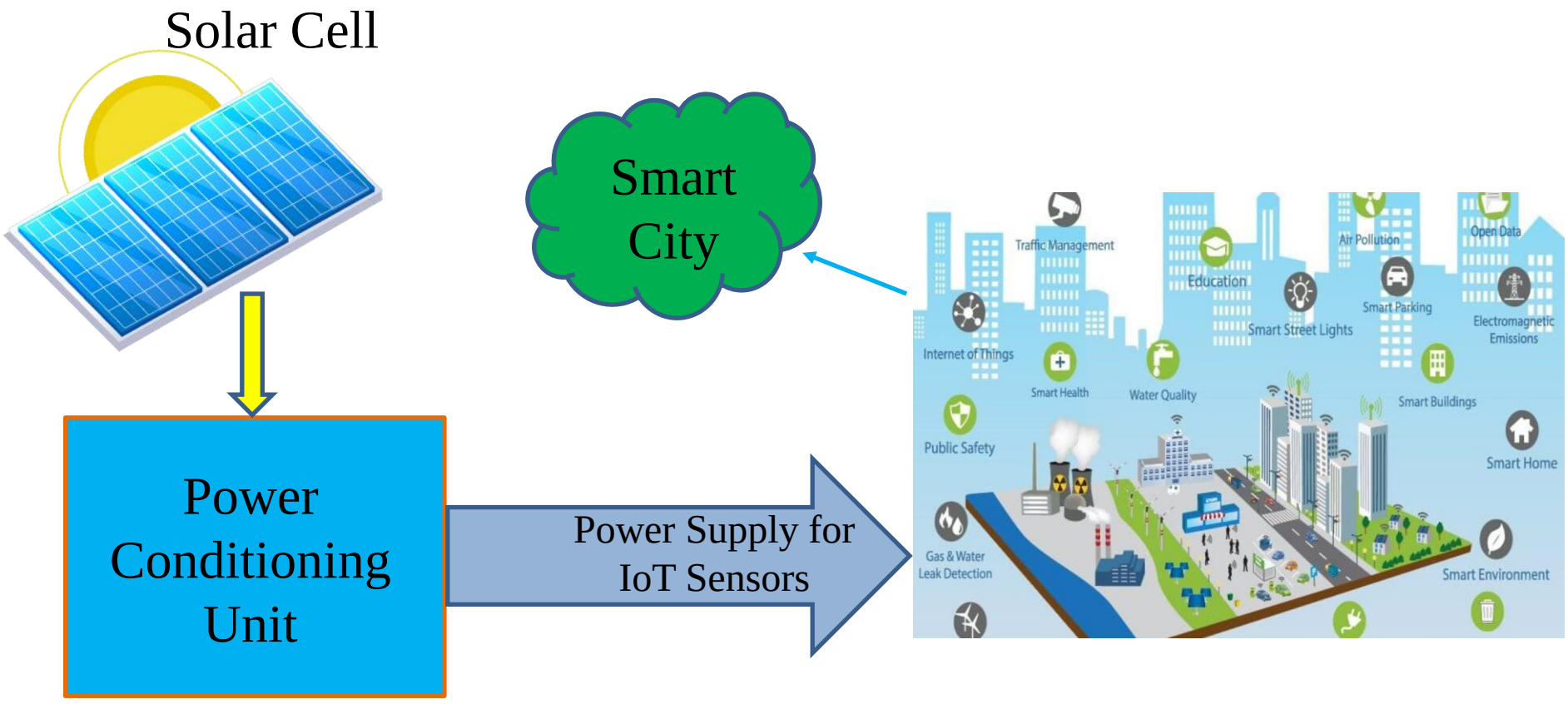

Fig. 1: Sustainable IoT in Smart Cities

Introduction Cond..

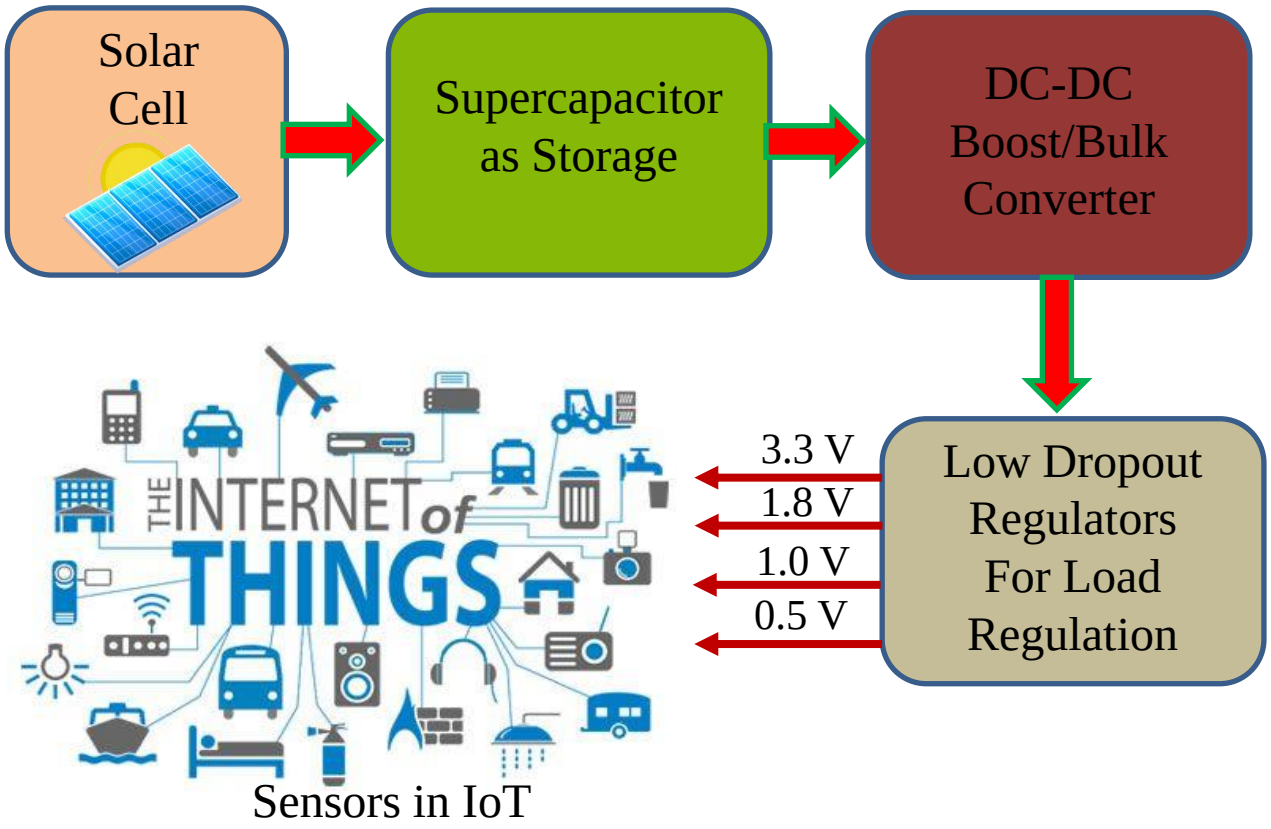

Fig. 2: Proposed PMU Concept for Sustainable IoT.

Novel Contribution of this Paper

- A solar cell-based energy harvesting and power management system is designed for sustainable IoT.

- Four different regulated power supplies of 0.5 V, 1 V, 1.8 V, and 3.3 V are generated targeting different sensors used in smart cities.

Proposed SEHS-PMU

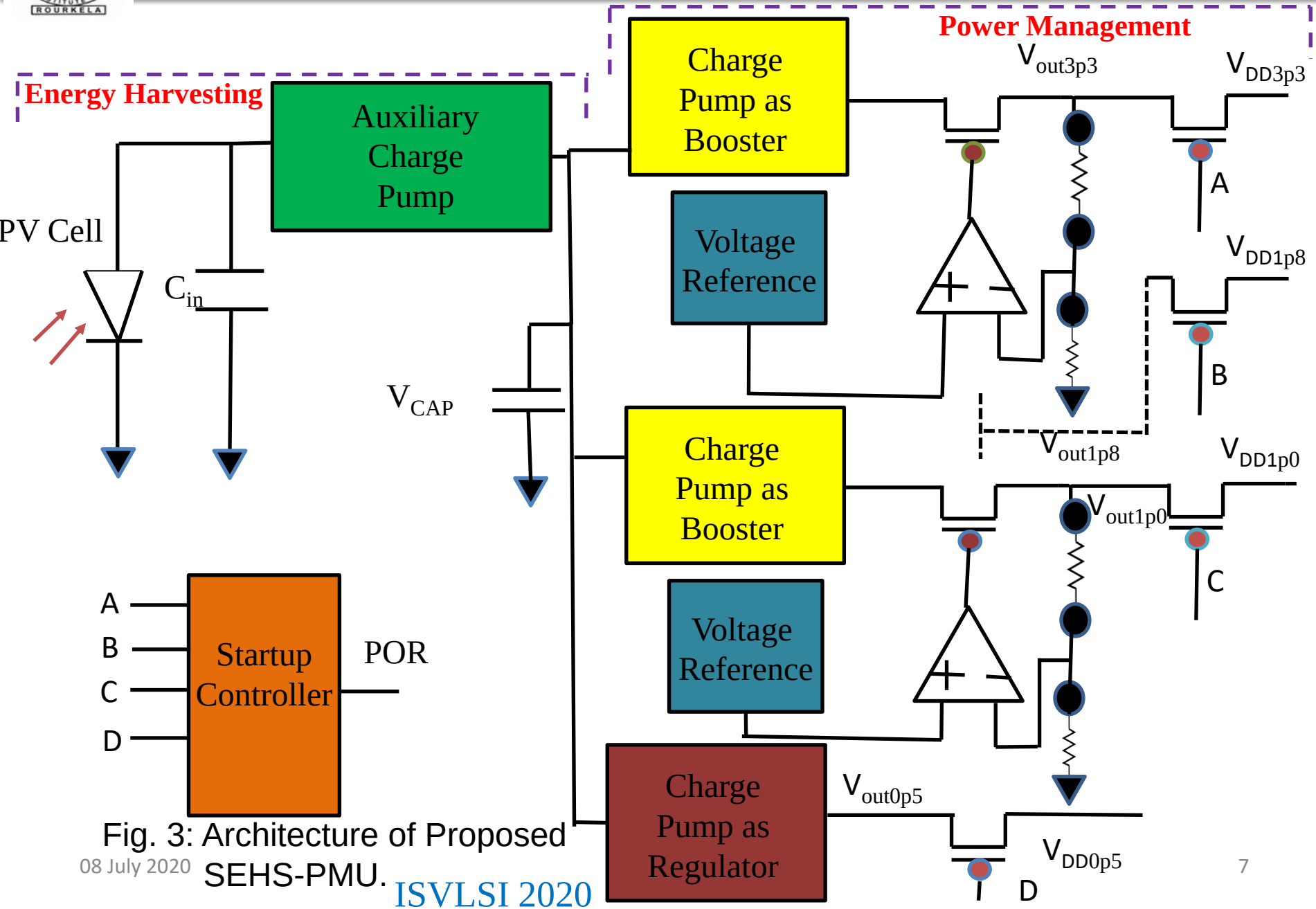

Fig. 3: Architecture of Proposed SEHS-PMU.

Dickson Charge Pump (DCP)

In Dickson charge pump the MOS devices function as diodes, so the current is unidirectional.

As shown in Fig. 4, two pumping clock pulses (*Clk* and *Clkbar*) are used which are in anti-phase with an amplitude of $V\varphi$.

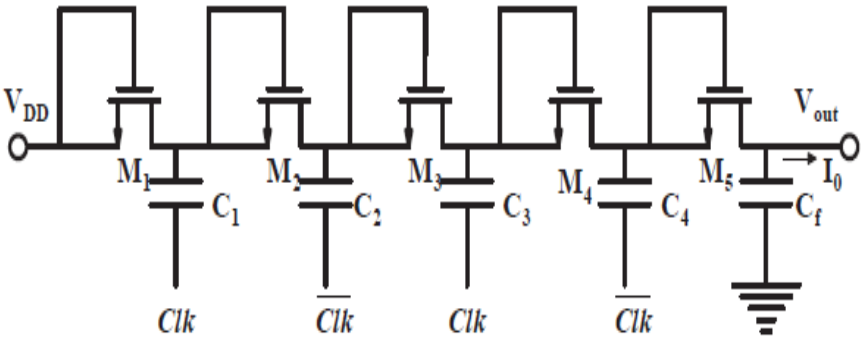

Fig. 4: Dickson Charge Pump.

The amplitude of the clock signal is the same as the supply voltage (V_{DD}).

The voltages are pumped into the circuit through the pumping capacitor C_1-C_4.

The voltage variation at each pumping node is expressed as described in the following expression:

$$\Delta V = V_{\phi}\frac{C}{C+C_s} - \frac{I_0}{f(C+C_s)}.$$

In the above expression, C is the capacitance of C_1-C_4, f is the clock frequency, C_s is the parasitic capacitance, I_0 is the output current.

Interleaved Switch Capacitor

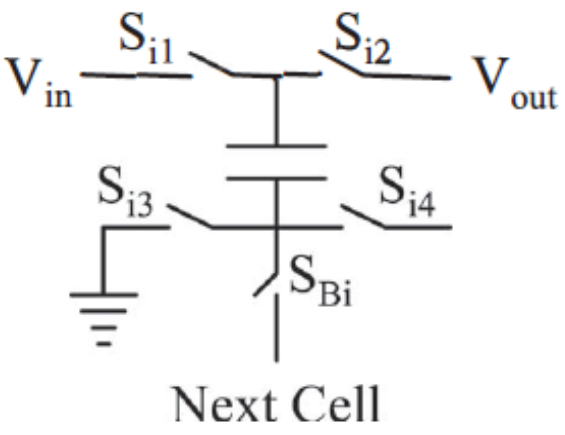

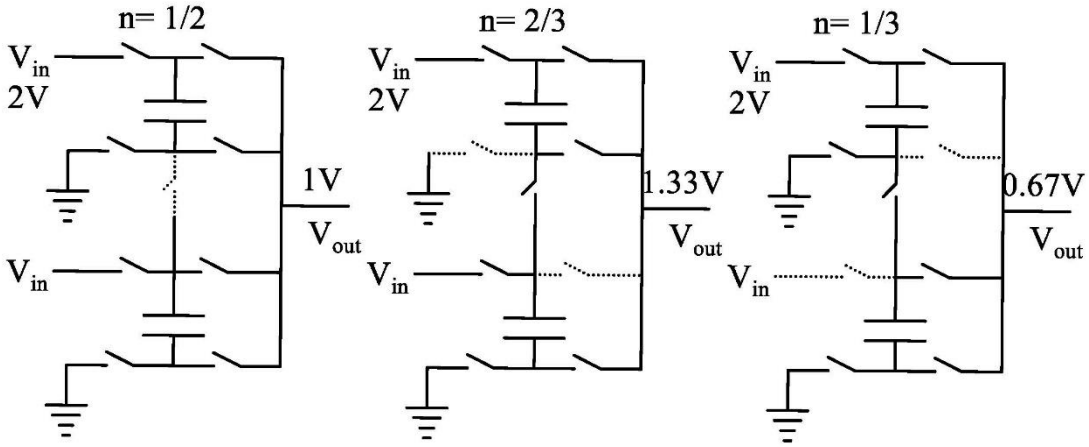

Fig. 5: Topology of a Standard Cell. Fig. 6: Interleaving Switched Capacitor.

Integrated capacitors/switches can be easily partitioned. The “Standard cell” configuration, as shown in Fig. 5 sets conversion ratio.
It also requires two non-overlapping clock pulses *Clk* and *Clkbar*. When *Clk* is High and *Clkbar* is Low:
capacitor is charged to (*Vin*-*Vout*). When *Clk* is Low and *Clkbar* is High: capacitor discharges to *Vout*. *Vout* is equal to (*Vin*-*Vout*), that gives *Vout*= 0.5 *Vin* as depicted in Fig. 6.

Band gap Reference Generator (BGR)

- A bandgap voltage reference is a temperature-independent voltage reference circuit widely used in integrated circuits. Circuit topology has been presented in Fig. 7.

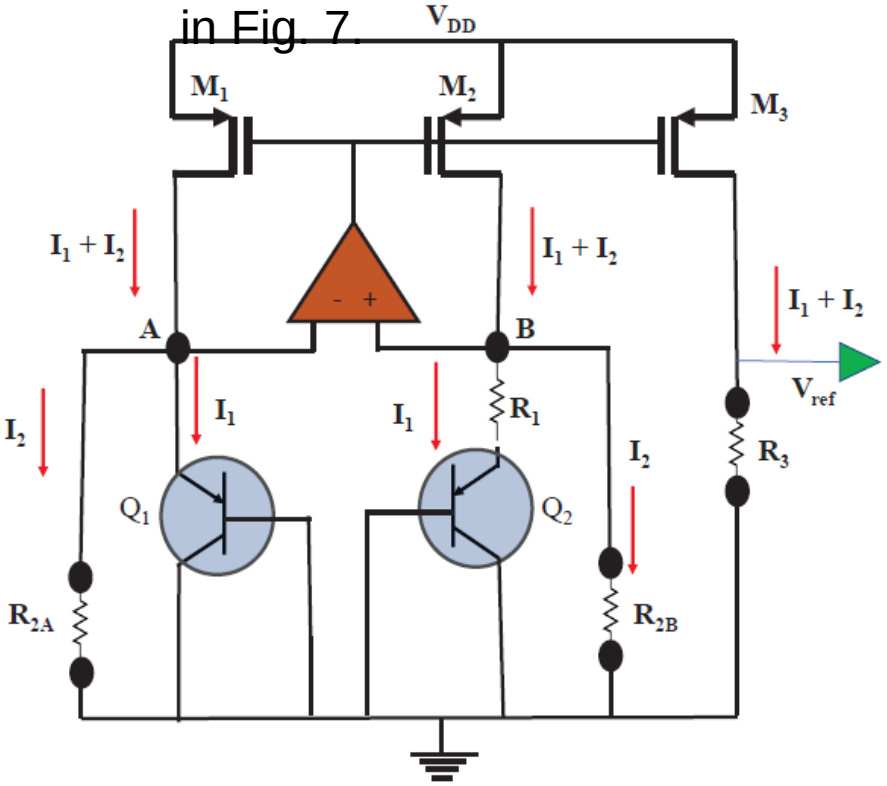

Fig. 7: Band gap Reference Generator

- It produces a fixed (constant) voltage regardless of power supply variations, temperature changes, and circuit loading from a device.
- It commonly has an output voltage around 1.25 V (close to the theoretical 1.22 eV (0.195 aJ) bandgap of silicon at 0 K).
- The voltage difference across resistor R_1 is positive temperature coefficient, so the current (I_1) passing through R_1 is considered as **Proportional to Absolute Temperature (PTAT).**
- The voltage at node A and node B is V_{be}, which is a negative temperature coefficient, so the current (I_2) passing through R_{2A} and R_{2B} is considered as a **Complementary to Absolute Temperature (CTAT)**.

- Adding both the currents, i.e., $I_1 + I_2$, a zero temperature coefficient current I_{ZTC} is obtained, which is mirrored using a current mirror circuit. By connecting a resistor R_3, the current obtained across it is I_{ZTC} and will provide a temperature-independent and power supply invariant reference voltage V_{ref}.

Low Dropout Regulator (LDO)

- A low-dropout regulator (LDO) is a DC linear voltage regulator that can regulate the output voltage even when the supply voltage is very close to the output voltage. The main components are a power FET and a differential amplifier (error amplifier).

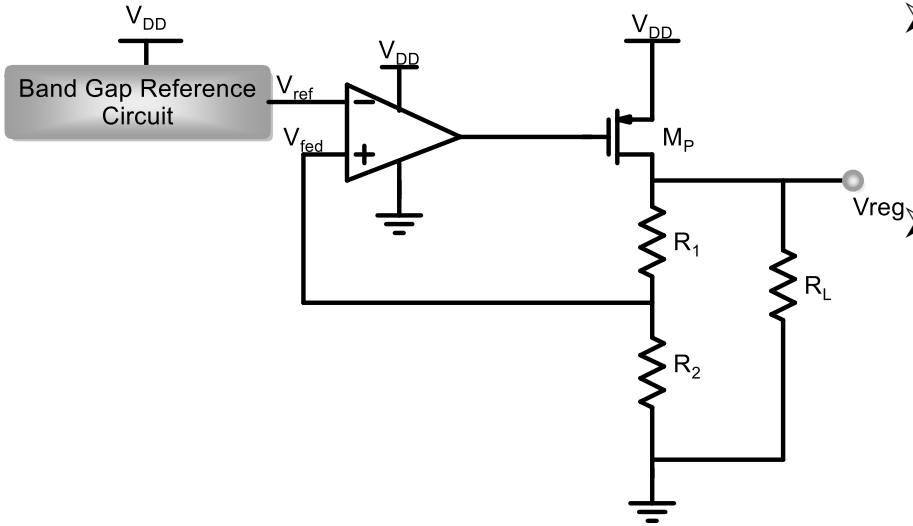

Fig. 8: Low Dropout Regulator (LDOs)

- One input of the differential amplifier monitors the fraction of the output determined by the resistor ratio of *R*1 and *R*2.
- The second input to the differential amplifier is from a stable voltage reference (bandgap reference). If the output voltage rises too high relative to the reference voltage, the drive to the power FET changes to maintain a constant output voltage.
- V_{out} depends on V_{ref}, R_1 and R_2. Changing R_1 and R_2 sets the output voltage.

Digital Controller

- The controller has a power-on reset (POR) mechanism, and a finite state machine (FSM) is used to select the loads as per the requirement to save power [21]. The four switching signals A, B, C, and D are meant for making ON/OFF the corresponding PMOS switches, as shown in Fig. 3.

Simulation Results

Simulation Results

The architecture discussed in this work were designed in CMOS 180nm technology library. A solar cell is used as an input source (with temperature 27◦C). The design specification

TABLE I: Design Characterization.

BGR Generator	**Error Amplifier**	**Converters**
I_{bias}=50μA	I_{tail}=50μA	Frequency = 10 MHz
V_{sgp}= 0.7 V	Unity Gain BW = 10 MHz	W/L Minimum
N= 4	0.8 < ICMR < 1.2	V_{CAP}=1.4 V
V_{ref}=0.9 V	Slew Rate=10 V/μS	C_f=1pF
V_{DD}=1.8 V	Phase Margin=60° and Gain=64dB	-

Simulation results of Regulated Outputs.

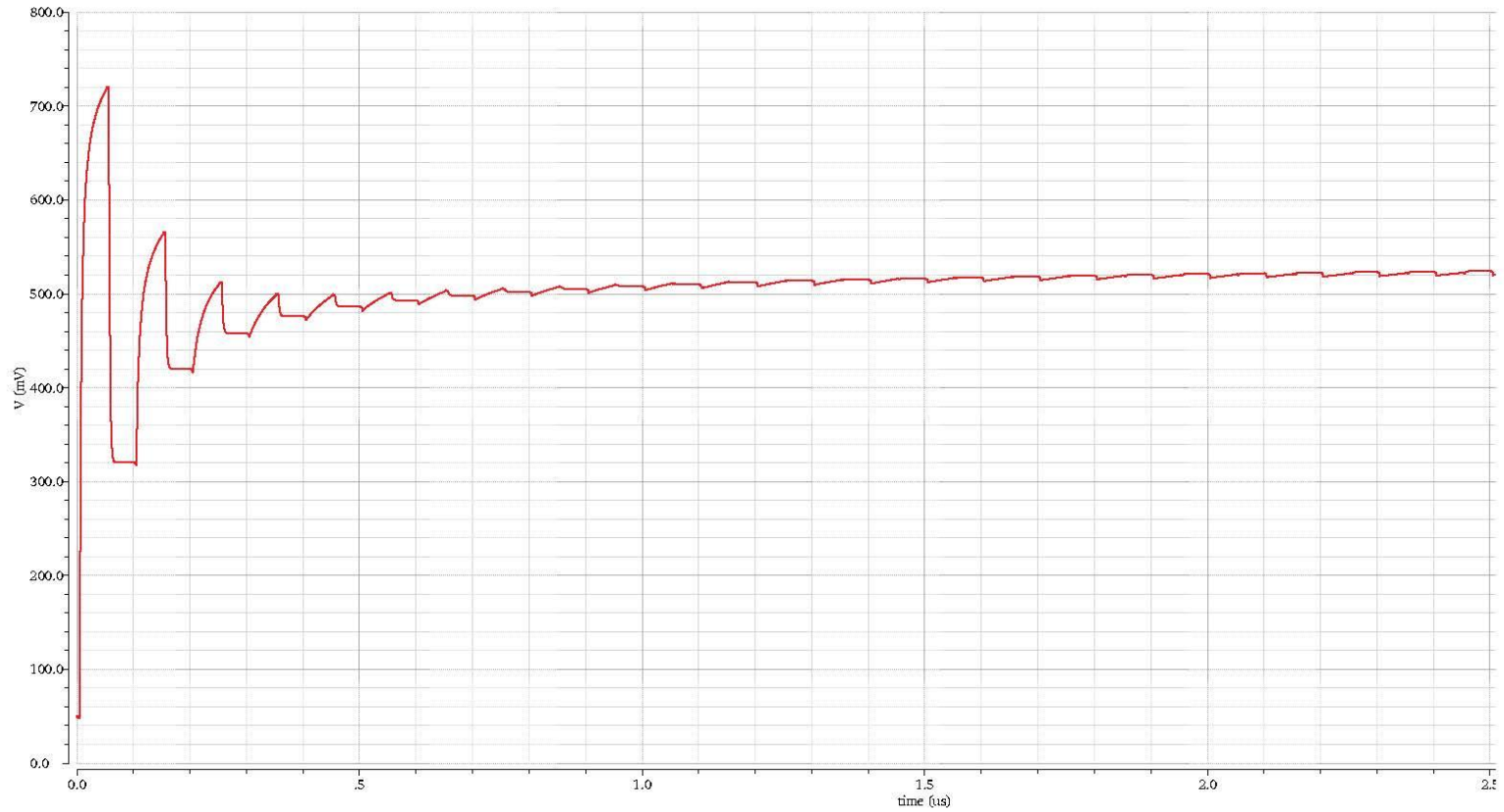

Fig. 9: Output of Two Way Interleaved Charge Pump.

Simulation results of Regulated Outputs from LDOs.

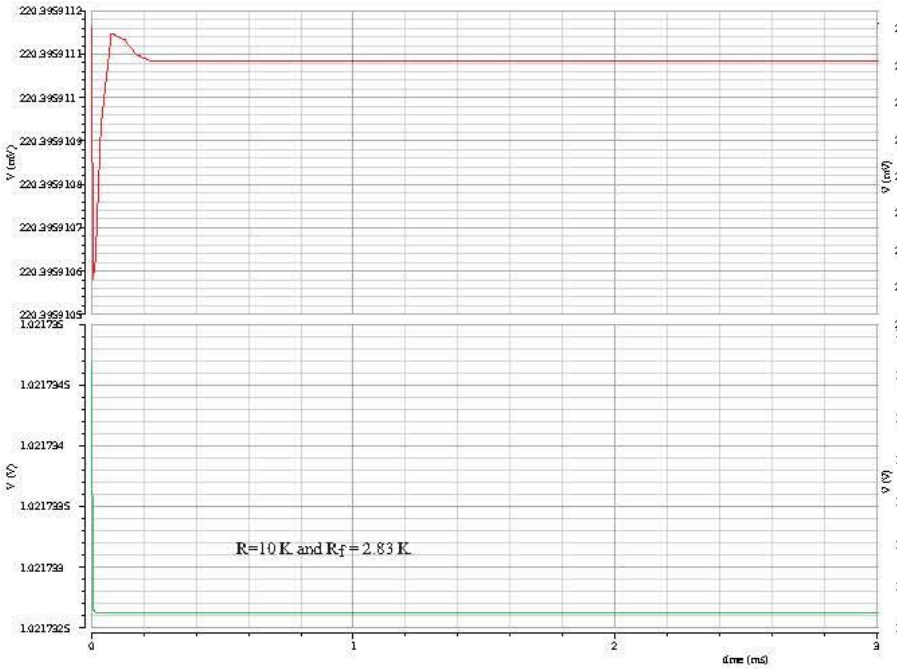

Fig. 10: Output of LDO V_{ref} = 1 V

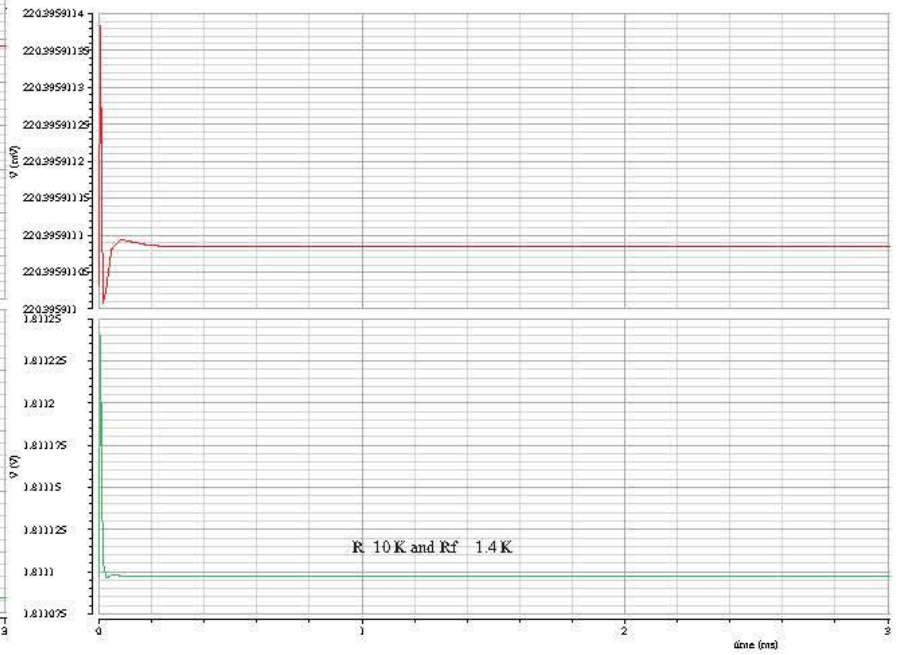

Fig. 11: Output of LDO V_{ref} = 1.8 V.

The value of R_1 is taken as 10 kΩ, and the feedback resistor (R_f) is 2.83 kΩ and 1.4 kΩ. The bandgap reference generator is providing a reference voltage of 220 mV.

Simulation results of Regulated Outputs from LDOs.

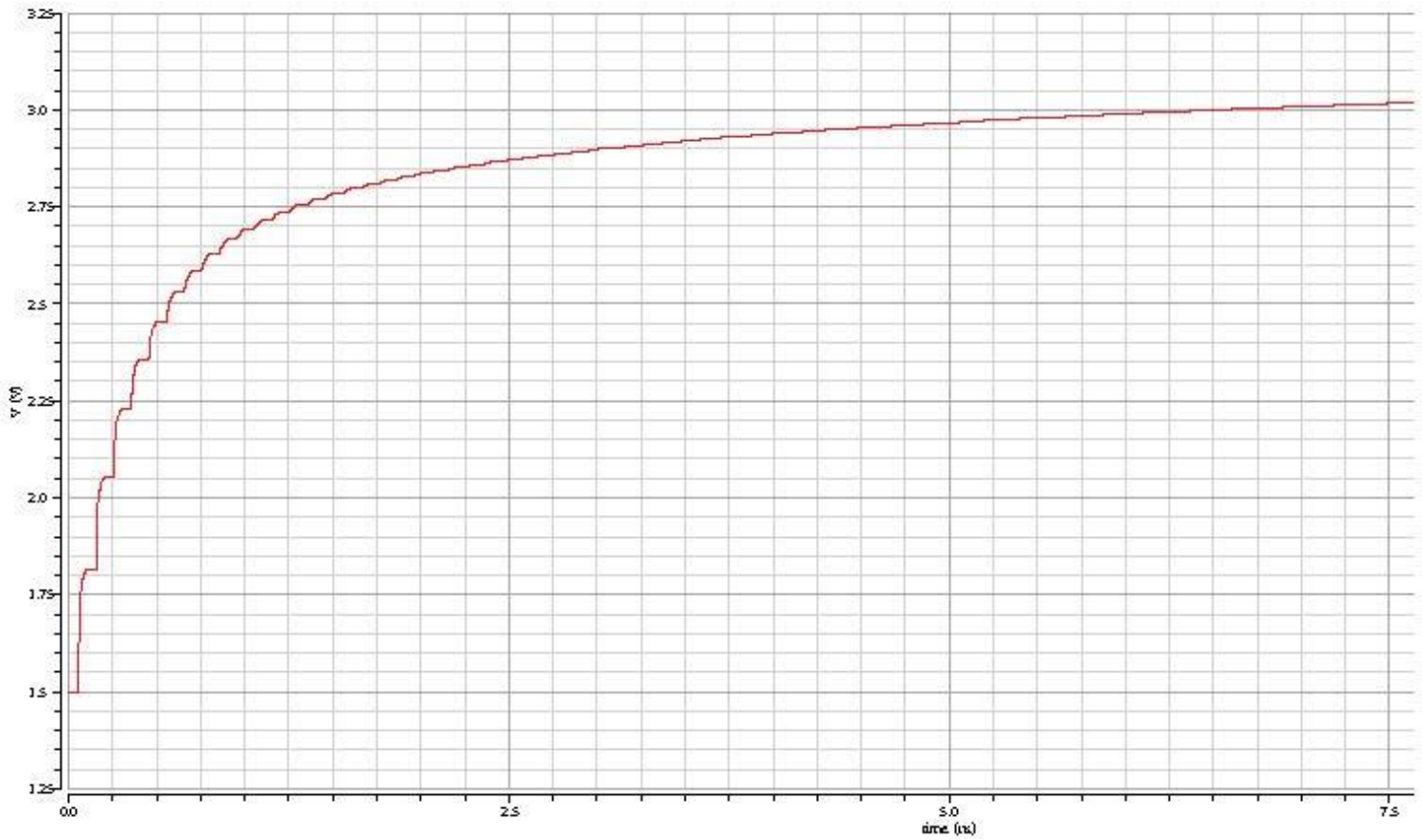

Fig. 12: Output of LDO V_{ref} = 3.3 V.

Simulation results of Regulated Outputs from LDOs.

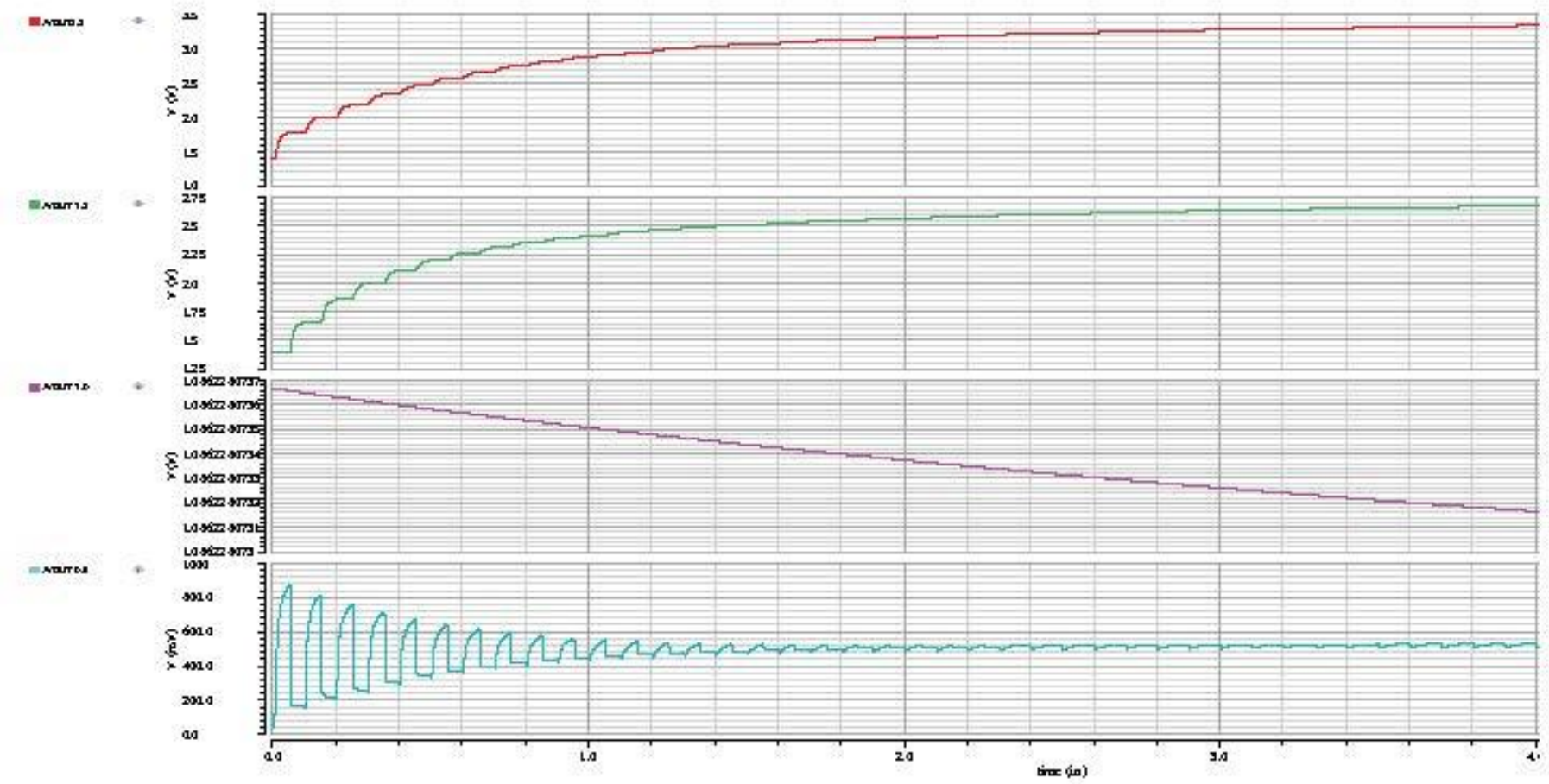

Fig. 13: Output of LDO *Vref* = 3.3 V, 1.8 V, 1 V and 0.5 V.

Comparison of Different Low Energy Harvesters

TABLE II: Comparison of different low energy harvesters.

Works	Feature/ Characteristics						
	Process	Source	Storage	Topology	No. of Outputs	Output Voltages	Load Power Range
Roy, et al. [9]	130nm	PV-TEG	Super-capacitor	Inductor + Super-capacitor	3	0.5 V, 1 V and 1.8 V	0-1mW@ 1 V, 0-500μW @0.5 V and 0-10μW @1.8 V
Klinefelter, et al. [11]	130nm	PV-TEG	Super-capacitor	Inductor	2	0.5 V and 1.2 V	0-5 mW
Jung, et al. [10]	180nm	Battery	Super-capacitor	-	3	0.6 v, 1.2 V and 3.3 V	20nW-500μW
Shih, et al. [8]	130nm	PV	Super-capacitor	-	1	1.4	0-12μW
Current Paper	180nm	PV	Super-capacitor	Super-capacitor	4	0.5 V, 1 V , 1.8 V and 3.3 V	0-1mW@ 1 V, 0-500μW @0.5 V, 0-10μW @1.8 V and 0-5μW @3.3 V

Conclusion

- The failure of sensor nodes in the IoT scenario can be a catastrophic situation in smart cities. A continuous power requirement is a must for IoT.

- Keeping these facts into consideration, the proposed SEHS-PMU is a self-sustainable solar EHS. It is a state of art technology towards clean energy and handling IoT end node devices in smart cities.

- The resulting regulated output voltages are 0.5 V, 1 V, 1.8 V, and 3.3 V, which is the requirement of many IoT edge node devices. The proposed SEHS-PMU is consuming power within the ultra-low-power range.

- The future directions of this research are to use the inherent features of the switched capacitors to design physically unclonable functionality (PUFs) and secure the devices used in IoT.

REFERENCES

[1] S. P. Mohanty, U. Choppali, and E. Kougianos, “Everything You wanted to Know about Smart Cities: The Internet of Things is the backbone,” *IEEE Consumer Electronics Magazine*, vol. 5, no. 3, pp. 60–70, July 2016.

[2] A. Omairi, Z. H. Ismail, K. A. Danapalasingam, and M. Ibrahim, “Power harvesting in wireless sensor networks and its adaptation with maximum power point tracking: Current technology and future directions,” *IEEE Internet of Things Journal,* vol. 4, no. 6, pp. 2104–2115, 2017.

[3] S. K. Ram, B. B. Das, A. K. Swain, and K. K. Mahapatra, “Ultra-Low-Power Solar Energy Harvester for IoT Edge Node Devices,” in Proc. IE*EE International Symposium on Smart Electronic Systems (iSES),* 2019, pp. 205–208.

[4] S. K. Ram, S. R. Sahoo, B. B. Das, K. K.Mahapatra, and S. P. Mohanty, “Eternal-Thing: A Secure Aging-Aware Solar-Energy Harvester Thing for Sustainable IoT,” *IEEE Transactions on Sustainable Computing*, no. 10.1109/TSUSC.2020.2987616, 2020.

[5] J. Katic, S. Rodriguez, and A. Rusu, “A high-efficiency energy harvesting interface for implanted biofuel cell and thermal harvesters,” *IEEE Transactions on Power Electronics*, vol. 33, no. 5, pp. 4125–4134, 2017.

[6] A. Shareef, W. L. Goh, S. Narasimalu, and Y. Gao, “A Rectifier-Less AC–DC Interface Circuit for Ambient Energy Harvesting From Low-Voltage Piezoelectric Transducer Array,” *IEEE Transactions on Power Electronics*, vol. 34, no. 2, pp. 1446–1457, 2019.

[7] S. Carreon-Bautista, A. Eladawy, A. N. Mohieldin, and E. S´anchez-Sinencio, “Boost converter with dynamic input impedance matching for energy harvesting with multi-array thermoelectric generators,” *IEEE Transactions on Industrial Electronics*, vol. 61, no. 10, pp. 5345–5353, 2014.

[8] Y.-C. Shih and B. P. Otis, “An Inductorless DC–DC Converter for Energy Harvesting With a 1.2 μW Bandgap-Referenced Output Controller,” *IEEE Transactions on Circuits and Systems II: Express Briefs*, vol. 58, no. 12, pp. 832–836, 2011.

Contd.

[9] A. Roy and B. H. Calhoun, “A 71% efficient energy harvesting and power management unit for sub-μW power biomedical applications,” in Proc. *IEEE Biomedical Circuits and Systems Conference (BioCAS)*, pp. 1–4, 2017.

[10] W. Jung, J. Gu, P. D. Myers, M. Shim, S. Jeong, K. Yang, M. Choi, Z. Foo, S. Bang, S. Oh et al., “8.5 A 60%-efficiency 20nW-500μW tri-output fully integrated power management unit with environmental adaptation and load-proportional biasing for IoT systems,” in Proc. *IEEE International Solid-State Circuits Conference (ISSCC),* 2016, pp. 154-155.

[11] A. Klinefelter, N. E. Roberts, Y. Shakhsheer, P. Gonzalez, A. Shrivastava, A. Roy, K. Craig, M. Faisal, J. Boley, S. Oh et al., “21.3 A 6.45 μW self powered IoT SoC with integrated energy-harvesting power management and ULP asymmetric radios,” in Proc*. IEEE International Solid-State Circuits Conference (ISSCC),* pp. 1–3, 2015.

[12] S. K. Ram, S. R. Sahoo, K. Sudeendra, and K. Mahapatra, “Energy efficient ultra low power solar harvesting system design with MPPT for IoT edge node devices,” in Proc. *IEEE International Symposium on Smart Electronic Systems (iSES),* pp. 130–133, Dec. 2018.

[13] S. K. Ram and B. B. Das, “Comparison of different control strategy of conventional and digital controller for active power line conditioner (APLC) for harmonic compensation,” in Proc. *12th International Conference on Environment and Electrical Engineering*, 2013, pp. 209–214.

[14] Z. H. Hsieh, N. X. Huang, M. S. Shiau, H. C. Wu, S.-Y. Yang, and D. G. Liu, “A novel mixed-structure design for high-efficiency charge pump,” in Proc. *16th International Conference Mixed Design of Integrated Circuits & Systems,* 2009, pp. 210–214.

[15] W. S. Ngueya, J. Mellier, S. Ricard, J.-M. Portal, and H. Aziza, “High voltage recycling scheme to improve power consumption of regulated charge pumps,” in Proc. *27th International Symposium on Power and Timing Modeling, Optimization and Simulation (PATMOS),* pp. 1–5, 2017.

[16] Z. Luo, M.-D. Ker, W.-H. Cheng, and T.-Y. Yen, “Regulated charge pump with new clocking scheme for smoothing the charging current in low voltage CMOS process,” *IEEE Transactions on Circuits and Systems I: Regular Papers,* vol. 64, no. 3, pp. 528–536, 2017.

Contd.

[17] G. Chen, H. Ghaed, R.-U. Haque, M. Wieckowski, Y. Kim, G. Kim, D. Fick, D. Kim, M. Seok, K. Wise et al., “A cubic-millimeter energy autonomous wireless intraocular pressure monitor,” in Proc. *IEEE International Solid-State Circuits Conference,* pp. 310–312, 2011.
[18] S. Bandyopadhyay, P. P. Mercier, A. C. Lysaght, K. M. Stankovic, and A. P. Chandrakasan, “A 1.1 nW energy-harvesting system with 544 pW quiescent power for next-generation implants,” *IEEE Journal of Solid-State Circuits*, vol. 49, no. 12, pp. 2812–2824, 2014.
[19] K. K. G. Avalur and S. Azeemuddin, “System Efficiency Improvement technique for Automotive Power Management IC using maximum load current selector circuit,” in Proc. *29th International Conference on VLSI Design and 2016 15th International Conference on Embedded Systems (VLSID),* pp. 240–245, 2016.
[20] M. Bedier, A. Karami, D. Galayko, and P. Basset, “Autonomous energymanagement interface for electrostatic series-parallel charge pump vibrational energy harvester,” in Proc. *15th IEEE International New Circuits and Systems Conference (NEWCAS)*, pp. 385–388, 2017.
[21] S. K. Ram and B. B. Das, “Digital controller design for three phase active power filter for harmonic and reactive power compensation using FPGA and system generator,” in Proc. *International Conference on Inventive Computation Technologies (ICICT),* vol. 3, pp. 1–6, 2016.

Queries…?

Contact: saswatram01@gmail.com

Thank You…